

A LINEAR MODELS APPROACH TO OPTIMIZE CARBAZOLE-BASED DYES FOR SOLAR CELL APPLICATIONS

Emanuel F. dos S. Mattos^a, Carlos R. A. Daniel^b, Nivan B. da Costa Júnior^{a}*

^aDepartment of Chemistry, Federal University of Sergipe Foundation, Sergipe,
49100-000, Brazil

^bDepartment of Statistics, Federal University of Sergipe Foundation, Sergipe,
49100-000, Brazil

*Corresponding Author: nivan@academico.ufs.br

DFT approach to selected modified dyes

The molecular structures of all molecules were optimized using Density Functional Theory (DFT) with the B3LYP functional and the 6-311G(d, p) basis set. Based on these optimized structures, the first 15 excited states were calculated using the CAM-B3LYP functional and the same basis set employed for the optimization. The ground and excited states for all molecules were obtained considering the solvent effect (chloroform) using the Conductor-like Polarizable Continuum Model (CPCM).

To simulate the interaction between the dyes and the semiconductor, we used the $(\text{TiO}_2)_9$ cluster due to its proven utility in other computational studies [1–5]. We considered the same bidentate binding mode because of its frequently reported stability [2–4]. Subsequently, the Dyes@ $(\text{TiO}_2)_9$ systems were optimized using the B3LYP functional with the 6-311G(d, p) and LANL2DZ basis sets, applying the latter exclusively to Ti atoms. The first 15 excited states were then calculated using the CAM-B3LYP functional and the two aforementioned basis sets. In addition, the solvent effect (chloroform) was considered in both calculations via the CPCM model.

Parameters related to photovoltaic properties

In DSSC research, it is notable that a significant amount of work has employed computational methods to evaluate potential new sensitizers, with Density Functional Theory (DFT) being the most frequent approach. This method is commonly used to explore parameters related to DSSC performance, such as J_{SC} and V_{OC} [6–8]. For instance, J_{SC} (Eq. S1) is related to the elementary charge, q , charge collection efficiency, η_{coll} , electron injection efficiency, η_{inj} , light-harvesting efficiency, $\text{LHE}(\lambda)$, and the photon flux from incident radiation, $I_s(\lambda)$.

$$J_{\text{SC}} = q \int \text{LHE}(\lambda) \times \eta_{\text{inj}} \times \eta_{\text{coll}} \times I_s(\lambda) d\lambda \quad \text{Eq. S1}$$

In this equation, the $\text{LHE}(\lambda)$ and η_{inj} can be evaluated by DFT methods. For example, a commonly employed approximation for $\text{LHE}(\lambda)$ involves only the oscillator strength, f , associated with the maximum absorption of the dye (Eq. S2).

$$\text{LHE} = 1 - 10^{-f} \quad \text{Eq. S2}$$

On the other hand, because directly estimating η_{inj} requires obtaining kinetic parameters related to charge injection and intramolecular decay [9,10], this term is

commonly assessed indirectly via the injection free energy, ΔG_{inj} , given their well-established satisfactory relationship ($\eta_{\text{inj}} \propto \Delta G_{\text{inj}}$) [9,10]. In this regard, ΔG_{inj} is readily obtained since it depends exclusively on the conduction band energy of the semiconductor, E_{CB} (-4.0 eV for TiO₂), and the oxidation potential of the dye in the excited state, E_{Dye}^* (Eq. S3). Where E_{Dye}^* depends on the vertical excitation energy for the maximum absorption, $E_{\lambda_{\text{max}}}$, and the oxidation potential of the dye in the ground state, E_{Dye} , which is essentially the negative of the HOMO energy (Eq. S4).

$$\Delta G_{\text{inj}} = E_{\text{Dye}}^* - E_{\text{CB}} \quad \text{Eq. S3}$$

$$E_{\text{Dye}}^* = E_{\text{Dye}} - E_{\lambda_{\text{max}}} \quad \text{Eq. S4}$$

A parameter related to the regeneration of the oxidized dye can also be estimated by obtaining the change in the regeneration free energy, ΔG_{reg} , a commonly used approach expressed by Equation S5. Here, $E_{I_3^-/I^-}$ corresponds to the redox potential of the I_3^-/I^- couple (-4.8 eV).

$$\Delta G_{\text{reg}} = E_{I_3^-/I^-} - E_{\text{Dye}} \quad \text{Eq. S5}$$

References

- [1] D. Fadili, Z.M.E. Fahim, S.M. Bouzzine, M. Hamidi, Improved photovoltaic performance of phosphonic acid-based sensitized solar cells via an electron-withdrawing moiety: A density of functional theory study, *Int J Quantum Chem* 121 (2021). <https://doi.org/10.1002/qua.26431>.
- [2] Y. Li, B. Xu, P. Song, F. Ma, M. Sun, D-A- π -A System: Light Harvesting, Charge Transfer, and Molecular Designing, *Journal of Physical Chemistry C* 121 (2017) 12546–12561. <https://doi.org/10.1021/acs.jpcc.7b02328>.
- [3] M. Gong, L. Zeng, W. Wang, X. Dong, Z. Yu, S. Wang, Y. Yang, Effects of Several Auxiliary Acceptors and Anchoring Groups on Charge Transfer and Photophysical Properties of D-A- π -A Type DSSCs: A DFT Study, *J Fluoresc* 35 (2025) 2285–2297. <https://doi.org/10.1007/s10895-024-03685-x>.
- [4] J. Zhang, Y.H. Kan, H. Bin Li, Y. Geng, Y. Wu, Z.M. Su, How to design proper π -spacer order of the D- π -A dyes for DSSCs? A density functional response, *Dyes and Pigments* 95 (2012) 313–321. <https://doi.org/10.1016/j.dyepig.2012.05.020>.
- [5] R. Sánchez-De-Armas, M.Á. San Miguel, J. Oviedo, J.F. Sanz, Coumarin derivatives for dye sensitized solar cells: A TD-DFT study, *Physical Chemistry Chemical Physics* 14 (2012) 225–233. <https://doi.org/10.1039/c1cp22058f>.
- [6] W. Zhang, L. Wang, L. Mao, J. Jiang, H. Ren, P. Heng, H. Ågren, J. Zhang, Computational Protocol for Precise Prediction of Dye-Sensitized Solar Cell Performance, *Journal of Physical Chemistry C* 124 (2020) 3980–3987. <https://doi.org/10.1021/acs.jpcc.9b10869>.

- [7] G. Consiglio, A. Gorcynski, S. Petralia, G. Forte, Computational study of linear carbon chain based organic dyes for dye sensitized solar cells, RSC Adv 13 (2023) 1019–1030. <https://doi.org/10.1039/d2ra06767f>.
- [8] D.D. Deng, J.K. Shi, J.X. Tong, F. Wang, X.L. Shi, J.Q. Li, W. Wei, Theoretical insights into single- and co-sensitization of indolocarbazole-based dyes on anatase (101) surface for efficient dye-sensitized solar cells, Comput Theor Chem 1247 (2025). <https://doi.org/10.1016/j.comptc.2025.115143>.
- [9] R. Katoh, A. Furube, Electron injection efficiency in dye-sensitized solar cells, Journal of Photochemistry and Photobiology C: Photochemistry Reviews 20 (2014) 1–16. <https://doi.org/10.1016/j.jphotochemrev.2014.02.001>.
- [10] R. Katoh, A. Furube, T. Yoshihara, K. Hara, G. Fujihashi, S. Takano, S. Murata, H. Arakawa, M. Tachiya, Efficiencies of Electron Injection from Excited N3 Dye into Nanocrystalline Semiconductor (ZrO₂, TiO₂, ZnO, Nb₂O₅, SnO₂, In₂O₃) Films, Journal of Physical Chemistry B 108 (2004) 4818–4822. <https://doi.org/10.1021/jp031260g>.
- [11] M. Hiiti Tsere, R. Costa, G. Deogratias, T. Pogrebnyaya, A. Pogrebnoi, R. Machunda, O.S. Al-Qurashi, N. Wazzan, N. Surendra Babu, Effect of Electron Donor Groups on Optoelectronic Properties of Betalain Dyes: A DFT Study, ChemistryOpen 14 (2025). <https://doi.org/10.1002/open.202400525>.
- [12] N. Kungwan, P. Khongpracha, S. Namuangruk, J. Meeprasert, C. Chitpakdee, S. Jungsuttiwong, V. Promarak, Theoretical study of linker-type effect in carbazole–carbazole-based dyes on performances of dye-sensitized solar cells, Theor Chem Acc 133 (2014) 1–14. <https://doi.org/10.1007/s00214-014-1523-4>.

Others result of free Dyes and Dye@(TiO_2)₉ systems

Structurally, all optimized complexes exhibit Ti–O bond lengths consistent with those obtained in other reported studies [11,12], falling within the range of 2.0 to 2.2 Å (see Table S1). Furthermore, given the negative energy for the interaction between the sensitizer and the (TiO_2)₉, E_{bind} (Eq. S6), it follows that the formation of the Dye@(TiO_2)₉ complex is favorable.

$$E_{\text{bind}} = E_{\text{Dye}@\langle \text{TiO}_2 \rangle_9} - (E_{\text{Dye}} + E_{\langle \text{TiO}_2 \rangle_9}) \quad \text{Eq. S6}$$

Table S1 – Bond lengths and interaction energy for the formation of the Dye@(TiO_2)₉ clusters.

Molecule	Ti-O1	Ti-O2	Energy bind(eV)
LY-F	2.192	2.055	-1.384
LY-P	2.059	2.245	-1.268
LY-S	2.180	2.073	-1.351
A1A2	2.071	2.194	-1.261
A1A5	2.148	2.096	-1.386
A1A6	2.163	2.069	-1.457
A3A1	2.175	2.091	-1.365
A3A4	2.149	2.091	-1.387
A6A3	2.173	2.092	-1.420

Figure S1. Frontiers molecular orbitals of HOMO and LUMO of the complexes Dye@(TiO_2)₉.

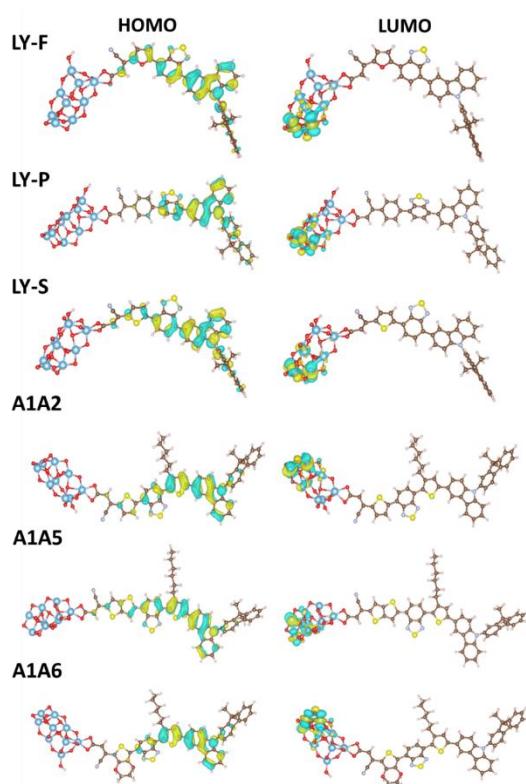


Table S2 – Energy (eV) of the HOMO, LUMO, and Gap for the Dye@ $(\text{TiO}_2)_9$ clusters.

Molecule	HOMO	LUMO	GAP
LY-F	-5.612	-3.455	2.157
LY-P	-5.606	-3.515	2.091
LY-S	-5.632	-3.464	2.167
A1A2	-5.437	-3.514	1.923
A1A5	-5.403	-3.478	1.924
A1A6	-5.444	-3.445	1.999

Table S3 – Absorption λ_{max} , oscillator strength and main compositions to Dye@ $(\text{TiO}_2)_9$.

Molecule	λ (nm)	f	Main Compositions*
LY-F	482.59	1.405	H-1 → L (15.52%) H → L (48.41%) H → L+1 (11.71%)
LY-P	411.67	1.235	H → L+2 (13.31%) H → L+3 (15.02%) H → L+8 (14.47%) H → L+9 (16.13%)
LY-S	464.02	1.530	H-1 → L (12.70%) H → L (38.90%) H → L+1 (13.83%)
A1A2	499.49	1.596	H-1 → L (18.97%) H → L (53.43%)
A1A5	502.62	2.033	H-1 → L (15.24%) H → L (42.14%)
A1A6	449.07	1.497	H-1 → L+1 (13.73%) H → L+1 (18.00%) H → L+2 (10.40%)

* H: HOMO, L: LUMO

Table S5. Dye Structures and Photovoltaic Performances

Dye	%PCE	Sol.	doi	Dye	%PCE	Sol.	doi
1.	5.64	Et	10.1016/j.tet.2013.02.058	33.	4.11	THF	10.1039/C3TA11748K
2.	4.22	Di	10.1021/am404948w	34.	6.40	THF	10.1039/C3TA11748K
3.	4.95	Di	10.1021/am404948w	35.	5.43	THF	10.1039/C3TA01657A
4.	6.04	Di	10.1021/am404948w	36.	6.50	THF	10.1039/C3TA01657A
5.	5.48	Di	10.1021/am404948w	37.	2.96	THF	10.1039/C3TA01657A
6.	1.21	Ac	10.1108/PRT-09-2014-0077	38.	4.61	THF	10.1039/C3TA01657A
7.	2.82	Ac	10.1108/PRT-09-2014-0077	39.	6.01	Di	10.1021/am508400a
8.	3.69	Ac	10.1108/PRT-09-2014-0077	40.	6.93	Di	10.1021/am508400a
9.	5.92	Ac	10.1016/j.jpowsour.2020.27776	41.	7.54	Di	10.1021/am508400a
10.	2.39	Tr	doi.org/10.1021/jp1055842	42.	3.64	Di	10.1002/ejoc.201300373
11.	2.48	Tr	doi.org/10.1021/jp1055842	43.	4.80	Di	10.1002/ejoc.201300373
12.	7.44	Tr	10.1016/j.electacta.2018.08.068	44.	5.69	Di	10.1002/ejoc.201300373
13.	3.50	Tr	10.1016/j.dyepig.2016.08.013	45.	4.62	Di	10.1002/ejoc.201300373
14.	2.68	Ac	10.1246/cl.2010.864	46.	1.77	Di	10.1016/j.dyepig.2012.03.028
15.	1.87	Di	10.1002/ejoc.201600353	47.	5.13	Di	10.1021/acsami.5b08888
16.	4.54	Di	10.1002/ejoc.201600353	48.	7.69	Di	10.1021/acsami.5b08888
17.	2.52	Di	10.1002/ejoc.201600353	49.	3.52	Di	10.1021/jp304489t
18.	4.57	Di	10.1002/ejoc.201600353	50.	4.10	Di	10.1021/jp304489t
19.	2.49	Tr	10.1016/j.solmat.2009.11.014	51.	5.12	Di	10.1021/jp304489t
20.	3.18	Tr	10.1016/j.solmat.2009.11.014	52.	3.34	Di	10.1016/j.solener.2018.09.073
21.	6.60	Tr	10.1016/j.tet.2014.01.001	53.	5.98	THF	10.1021/am5067145
22.	6.73	Tr	10.1016/j.tet.2014.01.001	54.	6.48	Di	10.1016/j.jpowsour.2015.01.148
23.	2.17	Tr	10.1039/C6RA01185C	55.	7.03	Di	10.1016/j.jpowsour.2015.01.148
24.	0.98	Tr	10.1039/C6RA01185C	56.	9.20	Di	10.1039/C3TA12368E
25.	2.69	Tr	10.1039/C6RA01185C	57.	7.15	Di	10.1039/C7NJ04629D
26.	0.98	Tr	10.1039/C6RA01185C	58.	7.26	Di	10.1039/C7NJ04629D
27.	1.11	Tr	10.1039/C6RA01185C	59.	0.57	Di	10.1007/s10854-018-9750-4
28.	5.78	Tr	10.1016/j.dyepig.2019.01.033	60.	0.92	Di	10.1007/s10854-018-9750-4
29.	5.23	Tr	10.1016/j.dyepig.2019.01.033	61.	6.44	Di	10.1016/j.dyepig.2015.07.034
30.	5.97	Tr	10.1016/j.dyepig.2019.01.033	62.	4.77	Di	10.1016/j.dyepig.2015.07.034
31.	6.09	THF	10.1039/C3TA11748K	63.	4.38	Di	10.1016/j.dyepig.2015.09.004
32.	5.55	THF	10.1039/C3TA11748K	64.	2.74	Di	10.1016/j.dyepig.2013.09.025

65.	2.94	Di	10.1016/j.dyepig.2013.09.0 25	96.	5.23	THF	10.1016/j.dyepig.2018.06.0 10
66.	4.30	Di	10.1016/j.dyepig.2013.09.0 25	97.	5.30	THF	10.1016/j.dyepig.2018.10.0 04
67.	4.86	Di	10.1016/j.dyepig.2013.09.0 25	98.	5.65	THF	10.1039/C3RA43057J
68.	6.25	Di	10.1016/j.jpowsour.2016.0 4.043	99.	6.23	THF	10.1039/C3RA43057J
69.	8.09	Di	10.1016/j.jpowsour.2016.0 4.043	100.	7.15	THF	10.1039/C3RA43057J
70.	6.98	Di	10.1016/j.jpowsour.2016.0 4.043	101.	5.20	THF	10.1039/C3RA43057J
71.	7.58	Di	10.1016/j.jpowsour.2016.0 4.043	102.	5.82	THF	10.1039/C3RA43057J
72.	7.50	Di	10.1039/C3RA22249G	103.	6.10	THF	10.1021/ol402931u
73.	7.01	Di	10.1039/C9TC01520E	104.	5.50	THF	10.1021/ol402931u
74.	8.01	Di	10.1039/C9TC01520E	105.	5.11	THF	10.1021/ol402931u
75.	5.06	Di	10.1039/C9TC01520E	106.	4.87	Di	10.1002/gch2.201900034
76.	4.23	DMF	10.1039/C7PP00350A	107.	4.49	THF	10.1039/C3TA12901B
77.	5.97	DMF	10.1039/C7PP00350A	108.	4.60	THF	10.1039/C3TA12901B
78.	5.34	DMF	10.1039/C7PP00350A	109.	3.03	THF	10.1002/asia.201402654
79.	5.02	Et	10.1016/j.tet.2006.12.082	110.	5.9	Tr	10.1039/C4QO00285G
80.	5.15	Et	10.1016/j.tet.2006.12.082	111.	6.5	Tr	10.1039/C4QO00285G
81.	3.87	Et	10.1016/j.tet.2006.12.082	112.	7.0	Tr	10.1039/C4QO00285G
82.	3.76	Et	10.1016/j.tet.2006.12.082	113.	4.31	Et	10.1021/jp906334w
83.	7.1	Et	10.1039/C5TA06548H	114.	5.96	Tr	10.1016/j.tet.2015.04.018
84.	8.48	Met	10.1016/j.dyepig.2018.03.0 72	115.	5.2	Di	10.1016/j.dyepig.2015.02.0 20
85.	4.69	Met	10.1016/j.dyepig.2018.03.0 72	116.	6.5	Di	10.1016/j.dyepig.2015.02.0 20
86.	4.65	THF	10.1016/j.dyepig.2012.10.0 02	117.	6.5	Di	10.1016/j.dyepig.2015.02.0 20
87.	3.96	THF	10.1039/C5RA02720A	118.	6.95	Di	10.1039/C4TA05162A
88.	2.85	THF	10.1039/C5RA02720A	119.	6.67	Di	10.1039/C4TA05162A
89.	7.52	THF	10.1039/C6TA02275H	120.	2.30	Di	10.1021/jo200501b
90.	8.51	THF	10.1039/C6TA02275H	121.	3.19	Di	10.1016/j.tetlet.2014.04.03 7
91.	7.58	THF	10.1016/j.dyepig.2016.12.0 13	122.	5.10	Di	10.1021/am500947k
92.	6.48	THF	10.1016/j.dyepig.2018.06.0 10	123.	4.90	Di	10.1002/cssc.201200975
93.	6.33	THF	10.1016/j.dyepig.2018.06.0 10	124.	5.80	Di	10.1002/cssc.201200975
94.	7.77	THF	10.1016/j.dyepig.2018.06.0 10	125.	5.80	Di	10.1002/cssc.201200975
95.	5.23	THF	10.1016/j.dyepig.2018.06.0 10	126.	5.60	Di	10.1002/cssc.201200975

Ac – Acetonitrile; **Et** – Ethanol; **Di** – Dichloromethane; **DMF** - Dimethylformamide; **Met** – Methanol; **Tr** – Trichloromethane; **THF** – Tetrahydrofuran;

